SIMULATION OF CERAMIC DPF MEDIA, SOOT DEPOSITION, FILTRATION EFFICIENCY AND PRESSURE DROP EVOLUTION

S. Rief (*), D. Kehrwald, K. Schmidt, A. Wiegmann
Fraunhofer-Institut Techno- und Wirtschaftsmathematik,
Fraunhofer-Platz 1, 67663 Kaiserslautern, Germany

ABSTRACT

Diesel particulate filters are gradually making their way into series production to keep emissions of fine dust to a minimum. But which filters are most efficient at extracting the noxious particles? How do the geometrical details of the filter material affect the filter properties? Until now, researchers and developers have to conduct series of tests to answer questions like these: They build prototypes, which then have to prove their abilities in experiments. The new simulation software **FilterDict** could in the future significantly reduce the number of prototypes, cutting time and cost of development – and offer some powerful new features, as well. For the first time, the 3D simulation software gives full insight into the filtration process. It allows simulating how fast and how far particles penetrate into the filter, for example – using any kind of filter material. As its input data, **FilterDict** requires a filter material model from the microstructure generator **GeoDict**, various physical parameters, and the particle size distribution. The program computes the path of the soot particles through the filter media. The simulation shows how much soot is deposited in which part of the filter and provides filter efficiency and pressure drop evolutions. Therefore, the design of the filter can be optimized to achieve long regeneration intervals, low fuel consumption and a high engine rating.

KEYWORDS

Diesel Particulate Filter, Emission Control, Filter Performance, Fine Dust Precipitation, Sintered Filter Media, Numerical Simulation

1 Virtual Sinter Structures

1.1 Structure Generation The generation of sinter structures comprises two steps: first, the stochastic object generator is used to create ellipsoids, cylinders and other basic geometrical shapes. In many applications this is done iteratively, e.g. large ellipsoids are generated which represent large pores, then, into the complement of the large ellipsoids smaller ellipsoids are generated which represent the initial grains of the sinter structure. At this stage, it is often a good idea to look at the shape and size distribution of the real sinter grains and try to match these distributions. During the second step, morphological operations [3] are applied to generate the sinter necks. Iteratively using the operations dilatation and erosion creates exactly the intended connectivity.

1.2 Comparison and Validation of Real and Virtual Structures For virtual structures which are intended to reproduce existing media quality measures are needed. Quite often, 2D SEM (= scanning electron microscope) images or even 3D tomography

data of a real sample are available. This information can be used to compute and compare various geometrical properties like porosity, cord length distributions, pore size distributions, specific surface area, anisotropies, etc. with **GeoDict** [4].
In industry, permeability tests of porous samples are standard. Moreover, flow simulations in typical porous media regimes, i.e. slow flow regimes are very reliable. Hence, measured and computed flow properties can be compared quite safely and provide meaningful results.

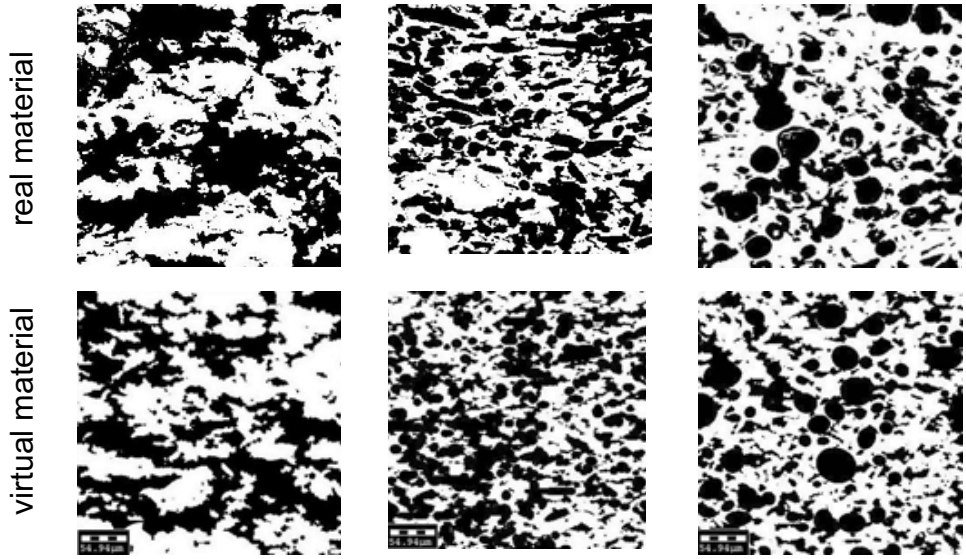

Fig. 1: 2D SEM images of real materials and 2D cross section images of the corresponding 3D reconstruction

2 Simulation of the Soot Filtration Process

2.1 Flow Computation Slow flow regimes are typical for most filtration processes. Hence, flow solvers for the solution of the Stokes or Stokes-Brinkmann equations are well-suited for the simulation. The Stokes-Brinkmann equations describe incompressible viscous flow in case of small velocities, i.e. when inertia is negligible. The Brinkmann-term takes into account the local permeabilities of deposited soot. The equations read:

$$-\mu\Delta\vec{u} + \mu K^{-1}\vec{u} + \nabla p = \vec{f}\text{, (conservation of momentum)} \quad (1)$$

$$\nabla\cdot\vec{u} = 0\text{, (conservation of mass)} \quad (2)$$

+ boundary conditions

In (1) and (2), μ, $\vec{u}$, K^{-1}, p, $\vec{f}$, denote the fluid viscosity, the velocity vector, the reciprocal of the permeability of deposited soot, the pressure and the external body force. In the free flow domain, the permeability K is infinite, simplifying (1), (2) to the Stokes equations

$$-\mu\Delta\vec{u} + \nabla p = \vec{f}\,, \quad (3)$$

$$\nabla\cdot\vec{u} = 0\,. \quad (4)$$

In regions with deposited soot, K^{-1} is typically quite large, and $\vec{u}$ is small. Therefore, the first term in (1) is negligible, and we obtain Darcy's law [1]

$$\vec{u} = -\frac{K}{\mu}(\nabla p - \vec{f}) . \tag{5}$$

2.2 Simulation of Particle Transport Certain assumptions can be made, simplifying the computation of the particle paths. This makes it possible to compute very large numbers of particles – which is necessary for realistic and meaningful simulations. The particles are spherical, there is no particle-particle interaction (= low particle concentration) and the particles do not influence the flow field as long as they are not deposited. After specifying the particle size distribution and a few additional parameters, particle motion is modeled by a Lagrangian approach

$$\frac{d\vec{v}}{dt} = -\gamma(\vec{v}(\vec{x}(t)) - \vec{u}(\vec{x}(t))) + \sigma\frac{d\vec{W}(t)}{dt}, \tag{6}$$

$$\frac{d\vec{x}}{dt} = \vec{v}, \tag{7}$$

where t, $\vec{x}$, and $\vec{v}$ denote time, position, and velocity of the particle, respectively. The first term on the right hand side of (6) describes the force due to friction. It is proportional to the difference of the particle velocity and the fluid velocity. The coefficient γ is given for slow flow and spherical particles by

$$\gamma = \frac{6\pi\mu R}{m} \text{ (Stokian friction)} \tag{8}$$

where R denotes the particle radius and m particle mass. The second term on the right hand side of (6) models Brownian motion by a three-dimensional Wiener-process $\vec{W}$. Let T be the temperature and k_B be the Boltzmann constant. Then we have by the fluctuation–dissipations theorem

$$\sigma^2 = \frac{2k_B\gamma T}{m} . \tag{9}$$

For further details of the model, we refer to [2]. For the solution of (6), (7), an implicit Euler method is applied.

2.3 Simulation of Particle Deposition Once a soot particle collides with the filter media it deposits. The deposited soot particles locally build up porous layers which affect the fluid flow via K as explained in 2.1. K is computed based on the volume fraction of deposited soot in a cell of the computational grid.
By alternately computing soot particle deposition and flow field, the build-up of the soot layers and the time dependent filter efficiency and pressure drop evolution are obtained. These are the quantities which are the target of the simulation and which developers of diesel particulate filters want to know.

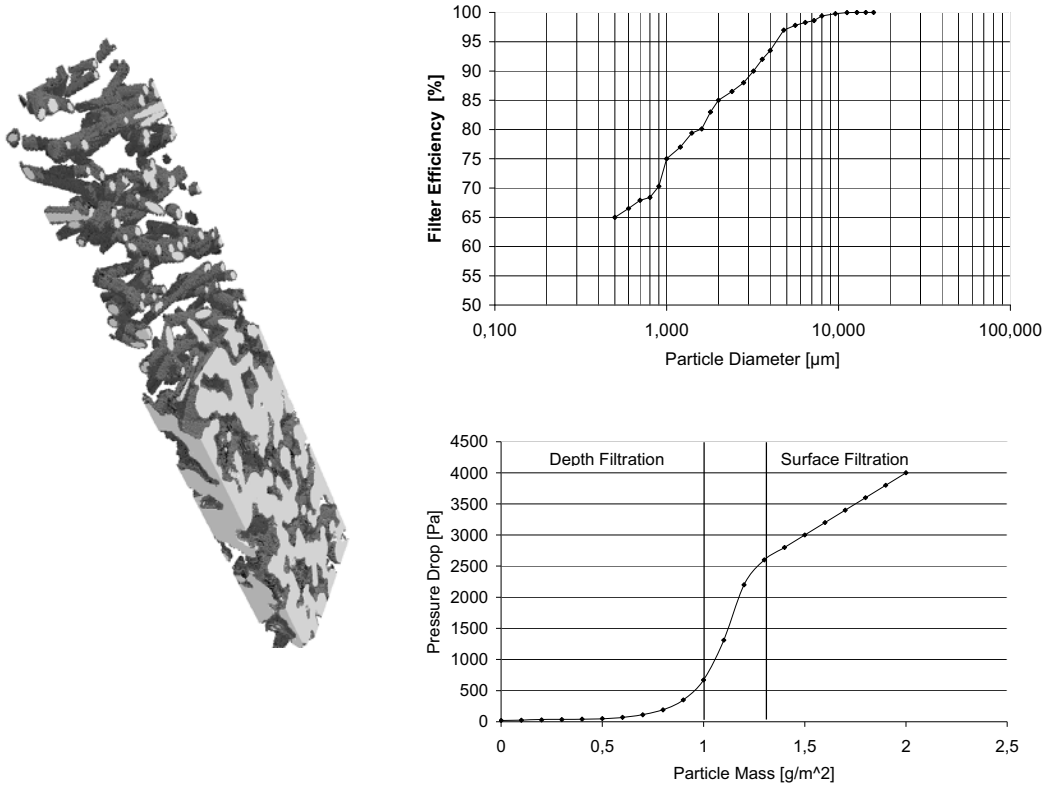

Fig. 2: Soot deposition, filter efficiency and pressure drop evolution computed by **FilterDict**

Runtime consumption and memory requirement of the flow computation limit the resolution of the computational grid to about 1 micron when a domain of about 300³ microns^3 is simulated. As the soot particles have diameters between 20 and 200 nanometers, one has to use an effective model for the deposition of soot particles inside the cells of the computational grid and for determining the point in time when the cell's filling capacity is reached.

2.3.1 The Volume Fraction Model The model deployed in **FilterDict** in the past was the volume fraction model. A floating point variable ρ states the filling degree with respect to soot for each cell. As long as a predefined maximum volume fraction $\rho_{\max}$ is not exceeded, particles can deposit inside the cell, thereby increasing the volume fraction ρ. Once ρ exceeds $\rho_{\max}$, the cell is considered to be filled and subsequent particles will deposit on its surface. The disadvantage of the volume fraction model is that the resulting shape of the soot layer can be far from reality as shown in Fig. 3. Once the soot layer has grown up wrongly, computations of the flow field and the pressure are not dependable anymore.

2.3.2 The Subgrid Model In the subgrid model, each cell which contains deposited soot particles is subdivided into several smaller cells. When a particle deposits, the cells of the subgrid located inside the particle are set to solid. Subsequent particles may deposit on preceding particles and a more realistic soot layer growth is achieved. The subgrid model needs ineffectually more runtime than the volume fraction model, but significantly more memory. For a simulation of a 300³ micron^3 domain up to 30GB

are needed. Memory of this extent can be addressed on a small cluster or will be deployable on 64 bit personal workstations at affordable prices in the not so far future.

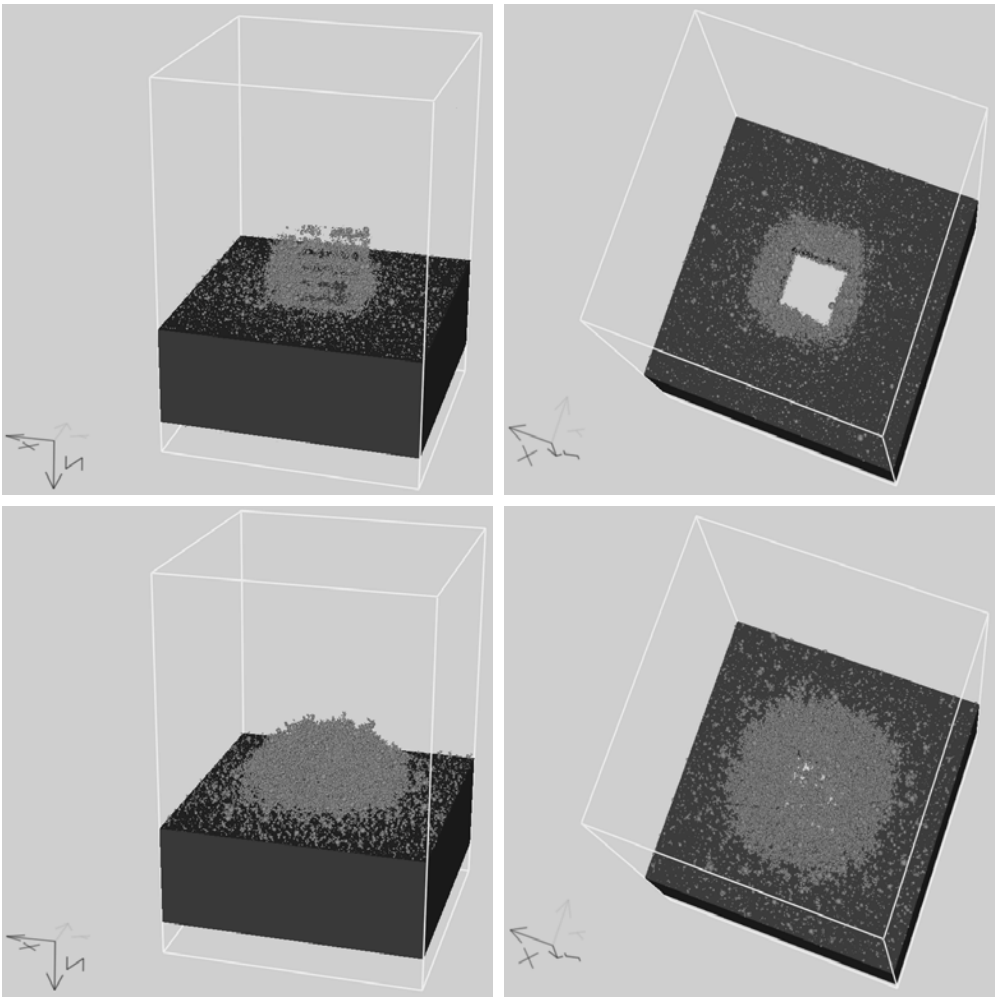

Fig. 3: Comparison of soot layer computed with volume fraction model (upper left and right) and subgrid-model (lower left and right) using a 16x16x23 grid with 1 micron resolution

Experiments show that the soot layer shapes computed with the subgrid model are very close to reality.

References

[1] Darcy, H.: “Les fontaines publiques de la ville de Dijon”, Dalmont, Paris, 1856.

[2] Latz, A.: “Partikel- und Wärmetransport durch Strömungen in Mikrostrukturen”, 2. Report, Stiftung Rheinland-Pfalz für Innovation, 2003.

[3] Ohser, J., Mücklich, F.: “Statistical Analysis of Microstructures in Materials Science”, John Wiley & Sons, 2000.

[4] Wiegmann, A.: GeoDict, Fraunhofer ITWM, http://www.geodict.com .